The following publication Kang Tan, Ying Huang, Guo-Qiang Lo, Chengkuo Lee and Changyuan Yu, "Three-dimensional polarization splitter and rotator based on multi-layer Si3N4-on-SOI platform," 2016 International Conference on Optical MEMS and Nanophotonics (OMN), Singapore, 2016 is available at https://doi.org/10.1109/OMN.2016.7565934.

Three-Dimensional Polarization Splitter and Rotator Based on Multi-Layer Si_3N_4-On-SOI Platform

Kang Tan,[1,2] Ying Huang,[1] Guo-Qiang Lo,[1] Chengkuo Lee,[2] and Changyuan Yu[2,3]

[1] *Institute of Microelectronics, A*STAR (Agency for Science, Technology and Research), 2 Fusionopolis Way, #08-02 Innovis Tower, Singapore 138634, Singapore*

[2] *Department of Electrical & Computer Engineering, National University of Singapore, Singapore 117583, Singapore*

[3] *Department of Electronic and Information Engineering, The Hong Kong Polytechnic University, Hung Hom, Kowloon, Hong Kong*

kang.tan@u.nus.edu

ABSTRACT

We propose a three-dimensional polarization splitter and rotator with high fabrication tolerance and CMOS BEOL compatibility, achieving a high TE-TE transmission and TM-TE conversion efficiency of -0.21dB and -0.63dB at 1310nm, respectively.

I. INTRODUCTION

As essential building block, polarization beam splitter and rotator (PSR) plays an important role in most photonic circuits where polarization handling is needed, including telecom, datacom, quantum integrated circuits, etc. [1] Different types of PSRs have been reported with various structures, such as Mach-Zehnder interferometer, directional coupler (DC) [2], slot waveguide and slab waveguide [3], etc.

In-plane DC has been successfully demonstrated as one of the simplest structures for achieving PSR [2]. The lack of solid upper cladding in this PSR breaks the vertical symmetry of strip waveguide, making polarization rotation achieved more easily. However, that also induces incompatibility and greatly complicates its integration with other building blocks based on most metal back-end-of-line processes. Hang Guan et al have proposed a PSR with SiO_2 as top cladding [3]; however the partial etching of cross waveguide reduced the fabrication tolerance. Wesley D. Sacher et al have reported a PSR consisting of a vertical coupler and a tapered silicon in-plane DC [4]. The complex architecture and long device length may limit its application in large-scale, highly-dense photonic integration.

In this work, we realize an O-band PSR by exploiting a simple 3-D structure with a Si_3N_4 strip waveguide placed in the upper right of a Si strip waveguide, which is enabled by multi-layer Si_3N_4-on-SOI platform [5]. Here we take the advantage of Si_3N_4 with lower refractive index to achieve easier phase matching as the TM mode in Si waveguide has a low refractive index, which enables the polarization splitting. Moreover, the freedom of Si_3N_4 waveguide location helps break both horizontal and vertical symmetry, making the polarization rotation possible. Therefore, this design can realize polarization splitting and rotating simultaneously, while silicon dioxide is able to be used as cladding for CMOS-compatible standard BEOL processes. Furthermore, the usage of Si_3N_4 contributes to better fabrication tolerance and broader bandwidth due to its material property [5]. Numerical simulations utilizing Lumerical FDTD solutions show that the present PSR has a high TM-TE conversion efficiency of -0.63dB and high TE-TE transmission efficiency of -0.21 dB at 1310nm, while the extinction ratio is 13.26dB and 16.31dB respectively. This work paves a way for better designs by utilizing Si_3N_4-on-SOI multi-layer platform.

II. PRINCIPLES AND DESIGN

Figure 1(a) shows the schematic structure. When TE mode is stimulated at the input port, the light beam keeps propagating along the silicon strip waveguide and then exit at the output port. This can be realized by setting a sufficient difference of effective indices between TE mode in the silicon strip waveguide and all possible modes in the Si_3N_4 strip waveguide, making phase-matching condition unsatisfied.

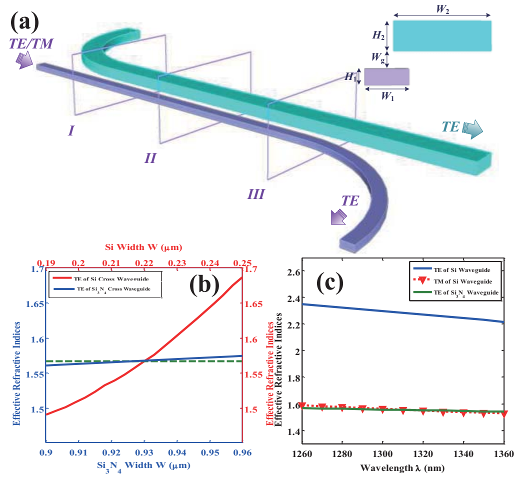

Fig. 1. (a) The PSR based on 3-D Si_3N_4-on-SOI structure. (b) The effective refractive index of TE mode in Si_3N_4 cross waveguide (blue line) matches that of the TM mode in Si waveguide (green line) when the width of Si_3N_4 cross waveguide is increasing. (c) The effective index of TM mode in Si waveguide matches well with that of the TE mode in Si_3N_4 waveguide over a wide wavelength range from 1260nm to 1360nm.

On the other hand, utilizing Si_3N_4 as the low refractive index material for cross waveguide naturally makes it easier to achieve the phase matching condition. Moreover, instead of putting cross waveguide in plane with the through waveguide, we exploit the position freedom provided by Si_3N_4 layer to place the Si_3N_4

cross waveguide on the top right of Si through waveguide, which naturally breaks both vertical and horizontal symmetries.

Here we design a sample for O-band wavelength based on a Si_3N_4-on-SOI platform developed by our group [5]. The silicon layer has a thickness H_1=150 nm and a width W_1= 420nm in order to let the waveguide support only fundamental modes operating at O-band. The height of Si_3N_4 is chosen as 280nm, compromising between the need to confine TE mode while ensuring large enough separation of refractive index between TE and TM mode. The width of Si_3N_4 can then be approximately calculated by utilizing phase matching condition. We firstly calculate the effective index of TM mode in Si waveguide which is depicted in green dashed line of Fig. 1(b), then the width of Si_3N_4 is swept to get an optimized value W_2= 930nm as shown by the blue line of the Fig. 1(b). Compared with the device using Si for cross waveguide demonstrated by the red line of the Fig. 1(b), the phase matching is much better for using Si_3N_4 as cross waveguide, indicating that using Si_3N_4 as cross waveguide is expected to achieve higher fabrication tolerance. Figure 1(c) shows that, using these designed parameters, the TM mode of Si through waveguide matches well with the TE mode of Si_3N_4 cross waveguide for 100 nm bandwidth. The vertical gap W_g between Si_3N_4 and Si determines the coupling efficiency and thus the device length, which is set to 170nm due to standard fabrication constraint. The length of coupling region is 63 µm for maximum light coupling. The horizontal shift S of Si and Si_3N_4 is then optimized as 530 nm for achieving highly efficient mode rotation.

III. SIMULATION RESULTS

We verify our design by exploiting three-dimensional finite-difference-time-domain method to simulate the light propagation along the PSR. When the TE mode is launched, the light beam is well confined and maintains its propagation in the Si waveguide as depicted in Fig. 2(a); while there is almost no light coupling from Si to Si_3N_4 waveguide, as depicted in Fig. 2(b). When TM mode is stimulated, the light beam is efficiently coupled to Si_3N_4 cross waveguide, while the mode is rotated from TM to TE at the same time, as shown in Fig. 2 (c) and (d). The PCE and extinction ratio of TM-TE for 1310nm is -0.63dB and 13.26dB, while the transmission efficiency and extinction ratio of TE-TE for 1310nm is -0.21dB and 16.31dB.

The TM mode splitting and rotating process is further demonstrated in Fig. 3. At cross section (II), the energy carried by TM mode starts to convert into TE mode in Si_3N_4 waveguide, as shown in Fig. 3(b). At cross section (III), light is mainly coupled to the Si_3N_4 waveguide, as depicted in Fig. 3(c). At the output of PSR, most of the power is carried by TE mode in the Si_3N_4 waveguide.

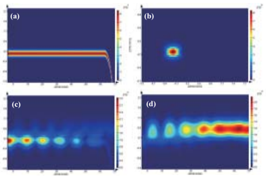

Fig. 2. (a) The light propagation in the Si layer and (b) cross section of both Si and Si_3N_4 waveguides at the end of the coupling region, when TE mode is stimulated at the Si input port. (c) The light propagation in the Si layer and (d) in the Si_3N_4 layer when TM mode is stimulated.

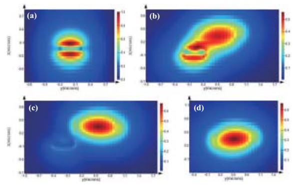

Fig. 3. The mode profile at the cross section I, II, III, and output port of Si_3N_4 waveguide.

IV. CONCLUSIONS

In summary, we have proposed a 3-D CMOS-compatible PSR operation at 1310nm, by utilizing only one Si_3N_4 strip waveguide and one Si strip waveguide constructed diagonally. Design optimization shows that such design is able to provide superior fabrication tolerance and bandwidth over its 2-D counter using only Si structure. Moreover, by exploiting the position freedom in the Si_3N_4 layer, the diagonal placing of Si_3N_4 cross waveguide naturally breaks both vertical and horizontal symmetries, which enables the use of SiO_2 as cladding to ensure compatibility with BEOL process for active integration. This proposal has the potential to be an essential building block for future multi-layer, high-density, CMOS-compatible photonic integrated circuits with polarization handling capability.

ACKNOWLEDGEMENT

This work was supported by the Science and Engineering Research Council of A*STAR Singapore. The SERC grant number is 1323300001.

REFERENCES

[1] T. Barwicz, M. R. Watts, A. Popovic Milos, P. T. Rakich, L. Socci, F. X. Kartner, E. P. Ippen, and H. I. Smith, “Polarization-transparent microphotonic devices in the strong confinement limit,” *Nat. Photonics*, vol. 1, pp. 57-60, 2007.

[2] L. Liu, Y. Ding, K. Yvind, and J. r. M. Hvam, “Silicon-on-insulator polarization splitting and rotating device for polarization diversity circuits,” *Opt. Express*, vol. 19, pp. 12646-12651 2011.

[3] H. Guan, A. Novack, M. Streshinsky, R. Shi, Q. Fang, A. E. Lim, G. Q. Lo, T. Baehr-Jones, and M. Hochberg,“CMOS-compatible highly efficient polarization splitter and rotator based on a double-etched directional coupler,” *Opt. Express*, vol. 22, pp. 2489–2496, 2014.

[4] W. D. Sacher, Y. Huang, D. Liang, T. Barwicz, J. C. Mikkelsen, B. J. F. Talyor, G.-Q. Lo, and J. K. S. Poon,“ Polarization rotator-splitters and controllers in a Si_3N_4-on-SOI integrated photonics platform,” *Opt. Express*, vol. 22, pp. 11167-11174, 2014.

[5] Y. Huang, J. Song, X. Luo, T.-Y. Liow, and G.-Q. Lo, “CMOS compatible monolithic multi-layer Si_3N_4-on-SOI platform for low-loss high performance silicon photonics dense integration,” *Opt. Express*, vol. 22, pp. 21859– 21865, 2014.